Supporting Information

Magnesium Halides as a Lead-free Family with Unique Optoelectronic Properties

Tingting Ye[1], Yunluo Wang[1], Shihao Ge[2], Tianrui Zhou[1], Jianghua Wu[2], Zesen Gao[1], Ruifeng Liu[1], ZeSheng Pan[1], Meiling Zhu[1], Jingshan Hou[2], Minghui Wang[3], Lianjun Wang[1,*], Haijie Chen[1,*], and Wan Jiang[1]

[1]*State Key Laboratory of Advanced Fiber Materials, Institute of Functional Materials, College of Materials Science and Engineering, Donghua University, Shanghai, 201620, P. R. China*

[2]*School of Materials Science and Engineering, Shanghai Institute of Technology, Shanghai, 201418, P. R. China*

[3]*Analysis and Testing Center, Donghua University, Shanghai, 201620, China*

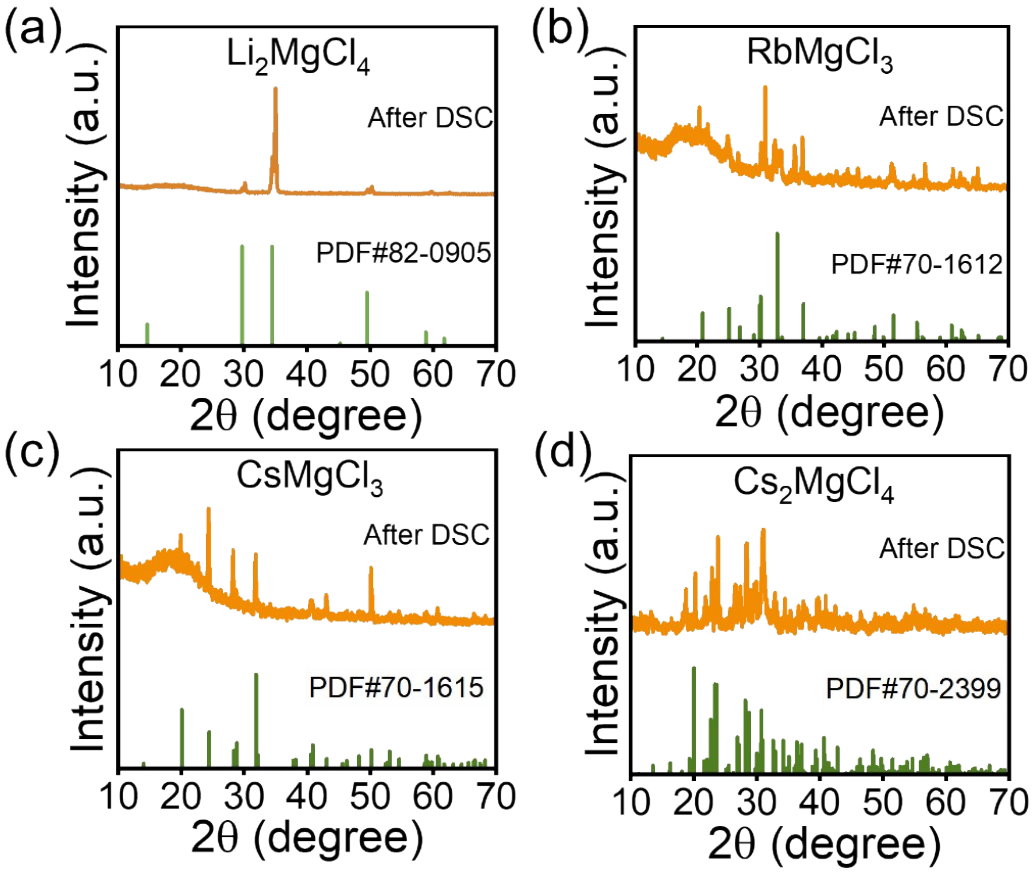

Figure S1. After DSC measurements, the PXRD spectra of (a) Li_2MgCl_4, (b) $RbMgCl_3$, (c) $CsMgCl_3$ and (d) Cs_2MgCl_4were compared with the standard cards.

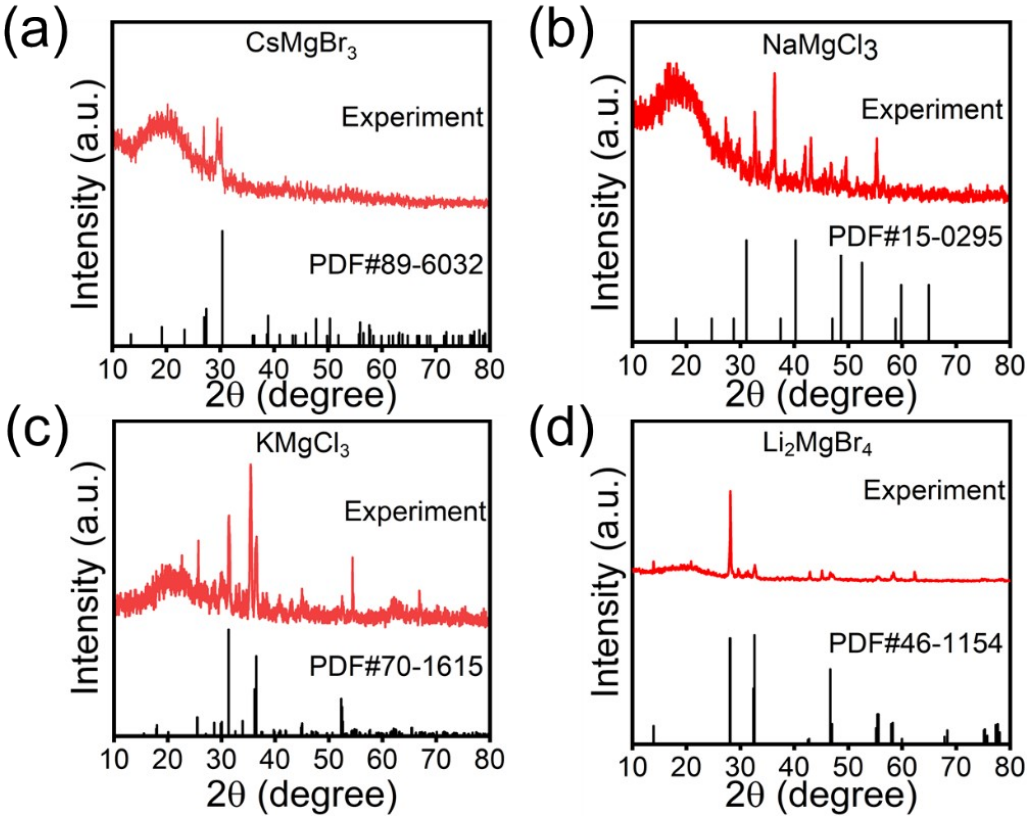

Figure S2. The PXRD patterns of (a) $CsMgBr_3$, (b) $NaMgCl_3$, (c) $KMgCl_3$ and (d) Li_2MgBr_4 were compared with standard cards.

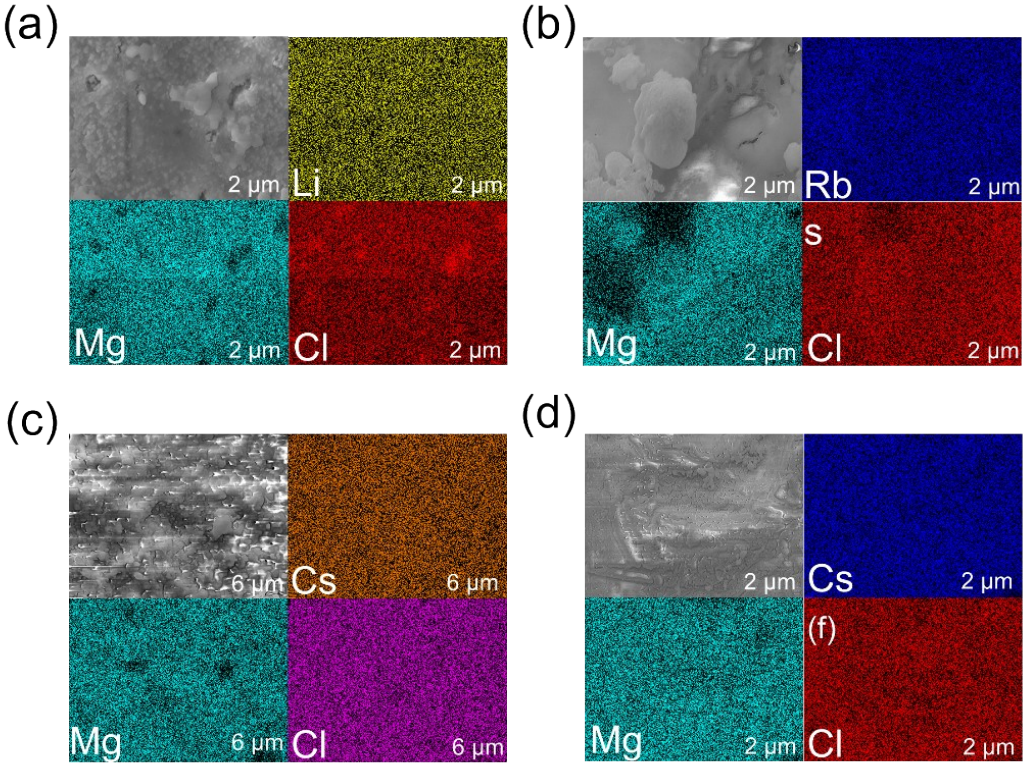

Figure S3. The SEM images and EDS elemental mapping of (a) Li_2MgCl_4, (b) $RbMgCl_3$, (c) $CsMgCl_3$ and (d) Cs_2MgCl_4.

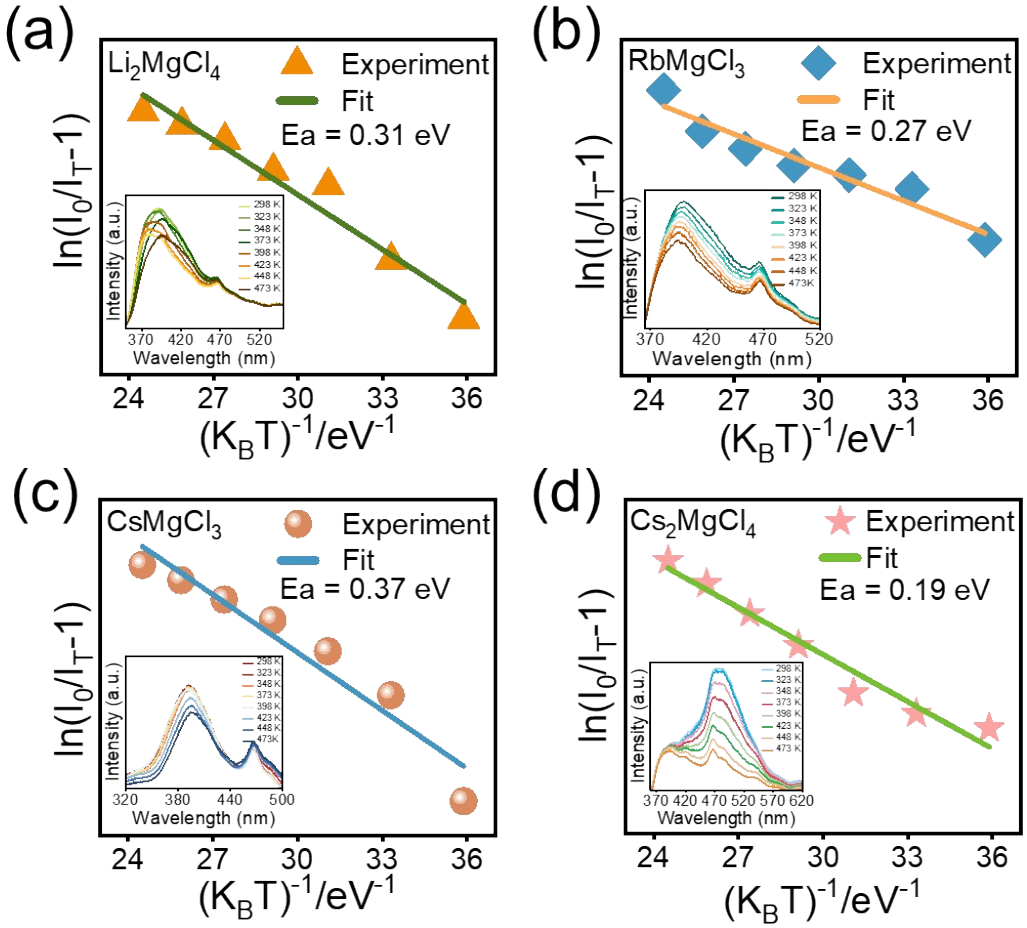

Figure S4. The relationship of ln[(I_0/I_T)-1] with 1/(k_BT) in (a) Li_2MgCl_4, (b) $RbMgCl_3$, (c) $CsMgCl_3$ and (d) Cs_2MgCl_4. (The inset are temperature-dependent PL spectra of (a) Li_2MgCl_4, (b) $RbMgCl_3$, (c) $CsMgCl_3$ and (d) Cs_2MgCl_4.)

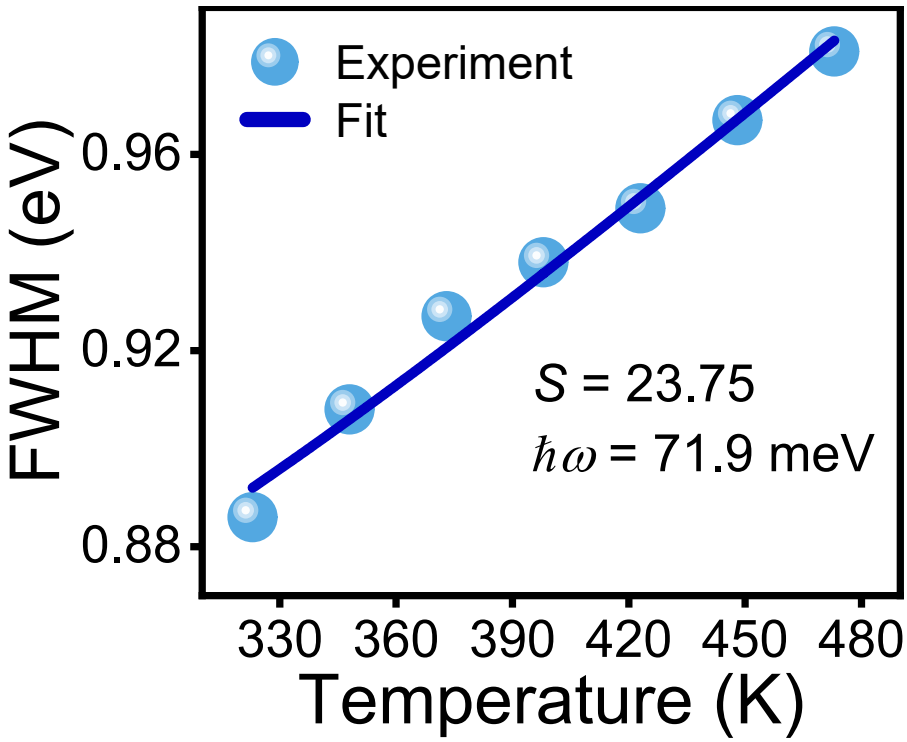

Figure S5. The correlation between integrated PL intensity and temperature.

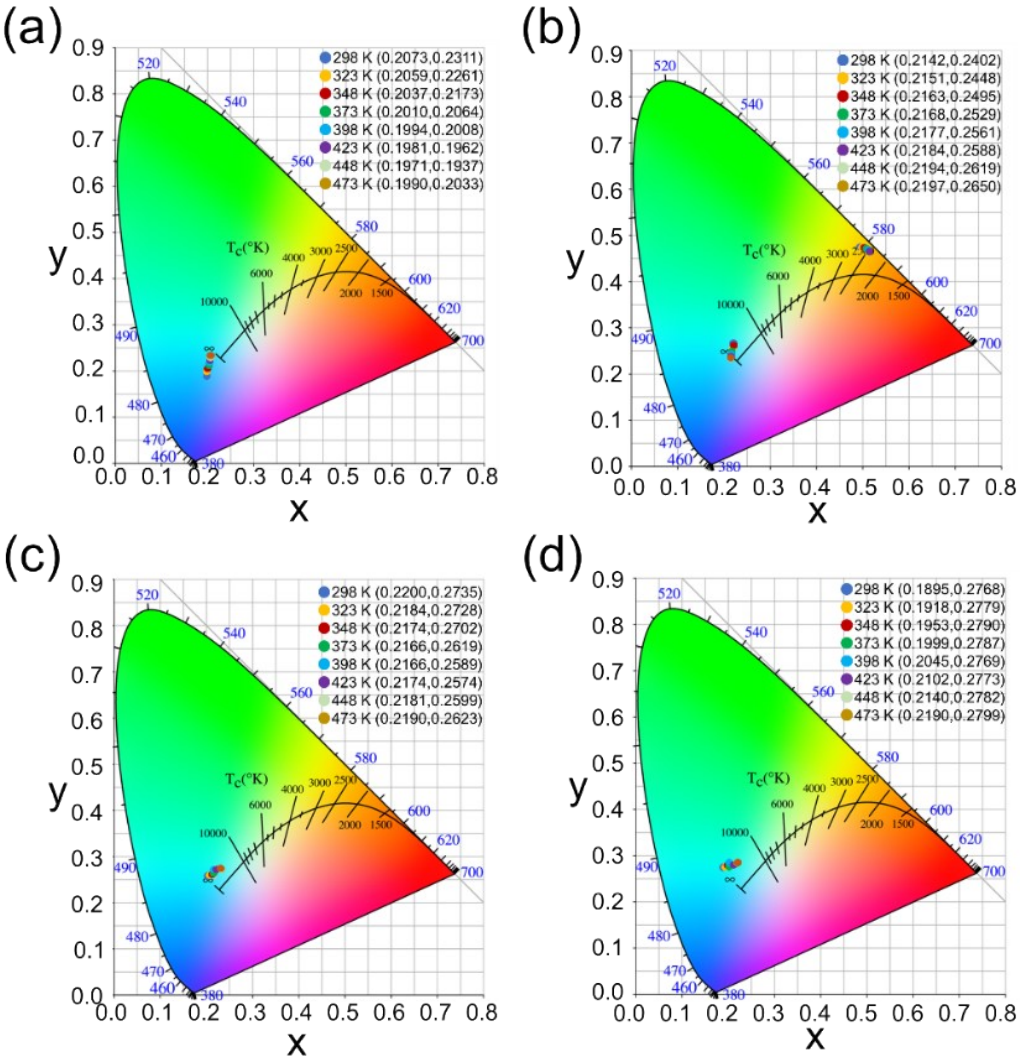

Figure S6. The CIE coordinates of PL in (a) Li_2MgCl_4, (b) $RbMgCl_3$, (c) $CsMgCl_3$ and (d) Cs_2MgCl_4 at different temperatures.

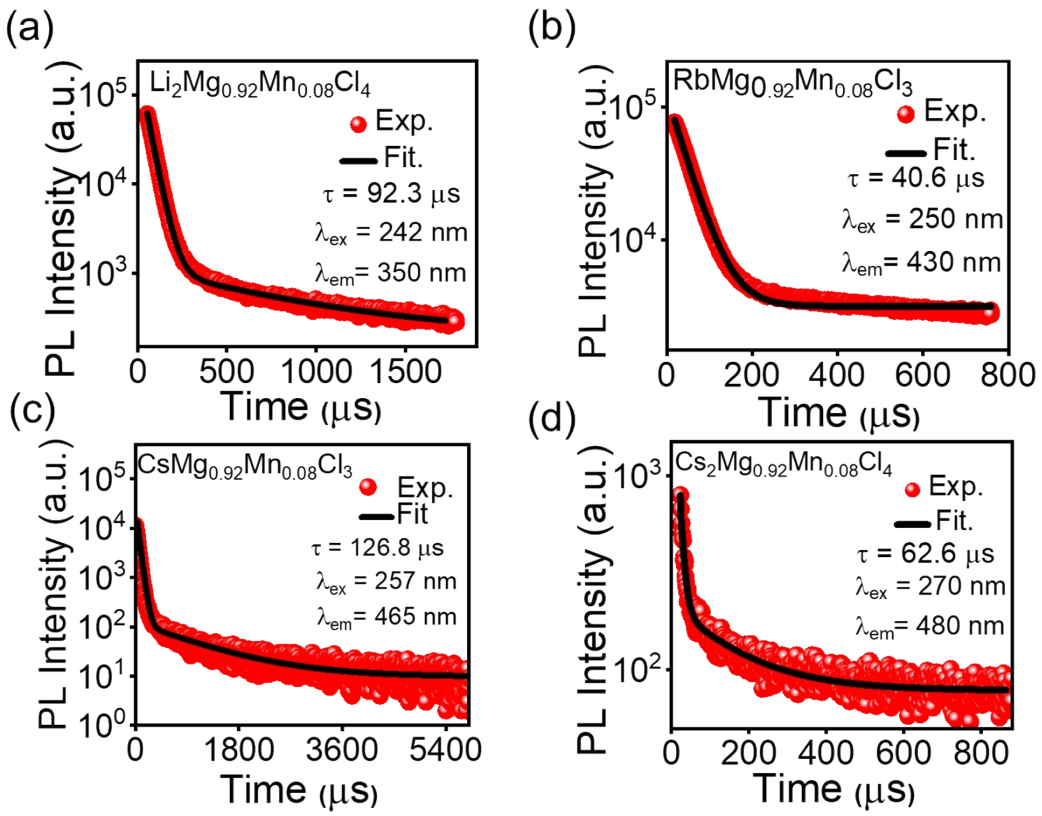

Figure S7. The PL decay curves of (a) $Li_2Mg_{0.92}Mg_{0.08}Cl_4$, (b) $RbMg_{0.92}Mg_{0.08}Cl_3$, (c) $CsMg_{0.92}Mg_{0.08}Cl_3$ and (d) $Cs_2Mg_{0.92}Mg_{0.08}Cl_4$. The fluorescence lifetime of the samples was calculated by using the single exponential equation: $y = y_0 + A_1 e^{-x/\tau}$.

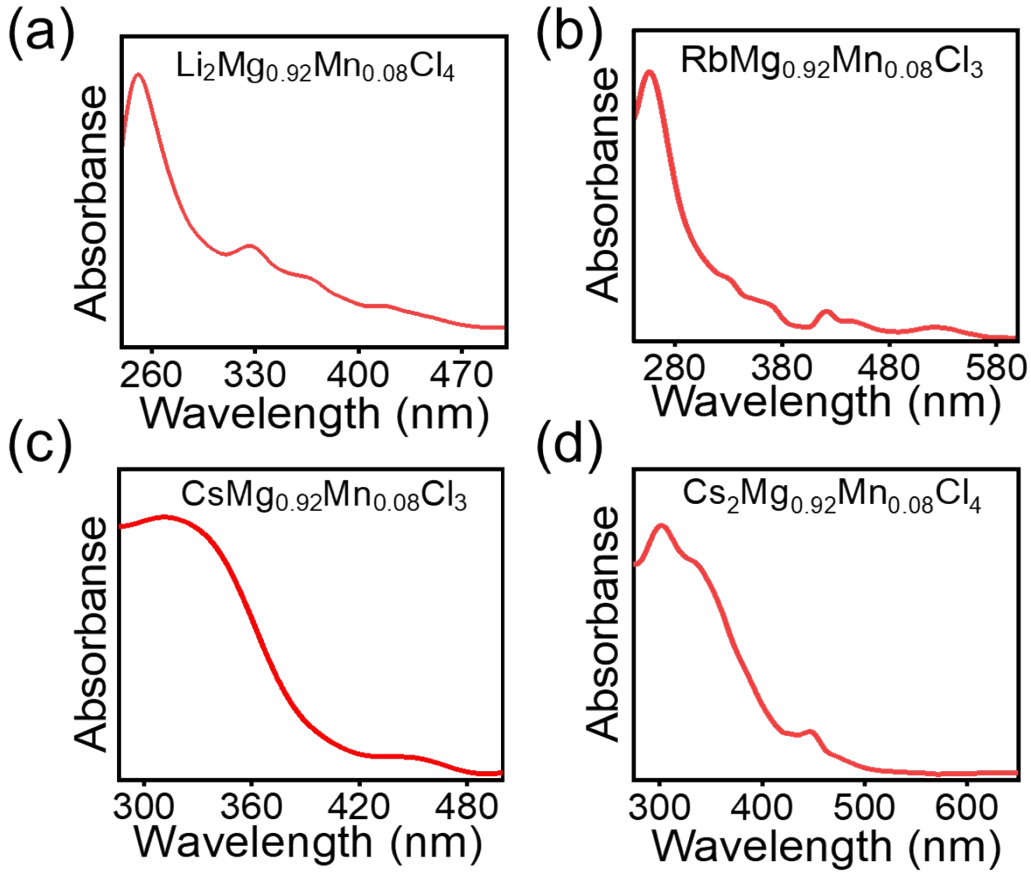

Figure S8. Absorption spectra of (a) $Li_2Mg_{0.92}Mg_{0.08}Cl_4$, (b) $RbMg_{0.92}Mg_{0.08}Cl_3$, (c) $CsMg_{0.92}Mg_{0.08}Cl_3$ and (d) $Cs_2Mg_{0.92}Mg_{0.08}Cl_4$.

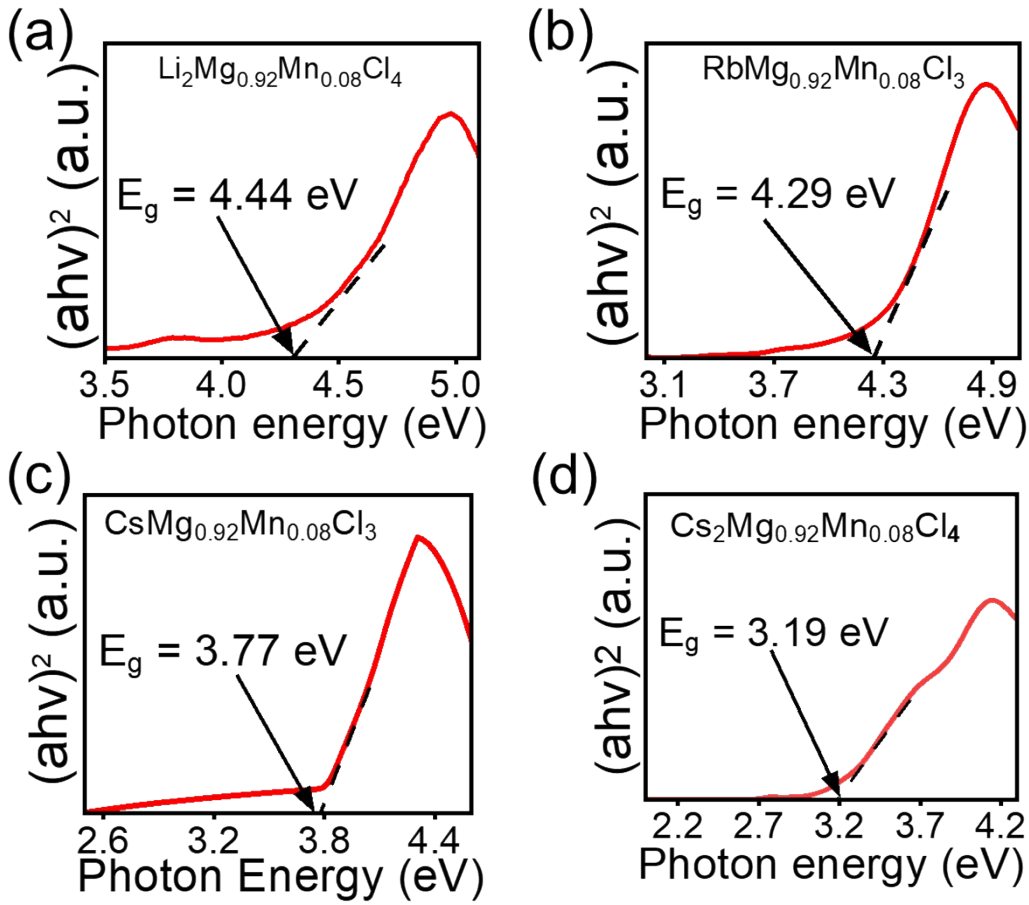

Figure S9. The Taua equation is used to calculate the optical band gaps of (a) $Li_2Mg_{0.92}Mg_{0.08}Cl_4$, (b) $RbMg_{0.92}Mg_{0.08}Cl_3$, (c) $CsMg_{0.92}Mg_{0.08}Cl_3$ and (d) $Cs_2Mg_{0.92}Mg_{0.08}Cl_4$.

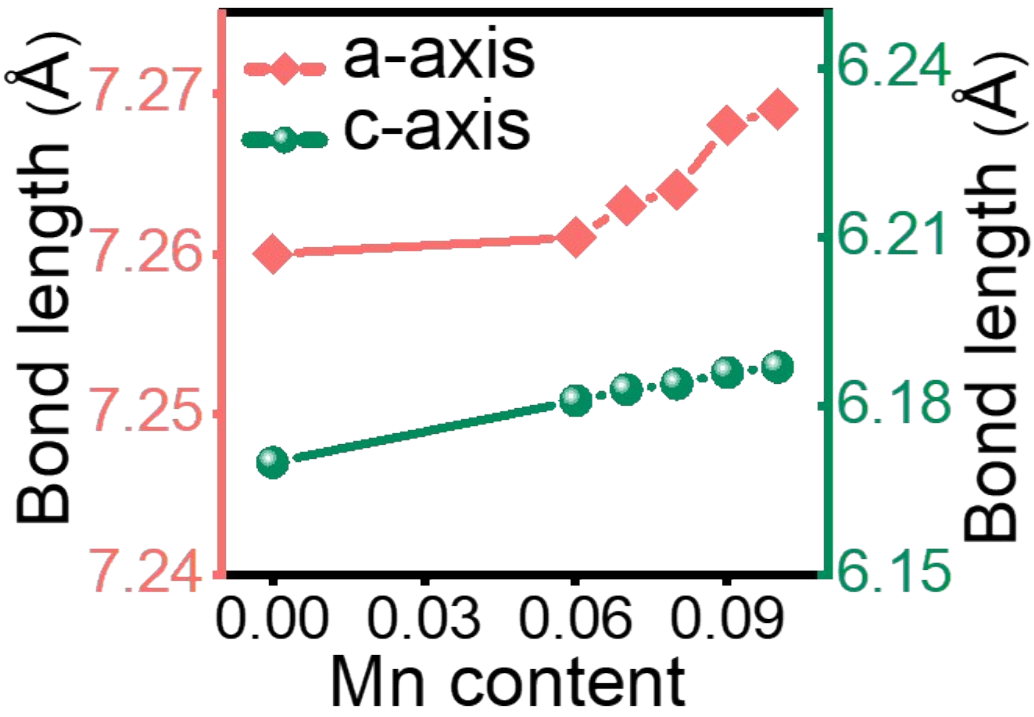

Figure S10. The change of cell constants of $CsMg_{1-x}Mn_xCl_3$ (x = 0 – 0.1).

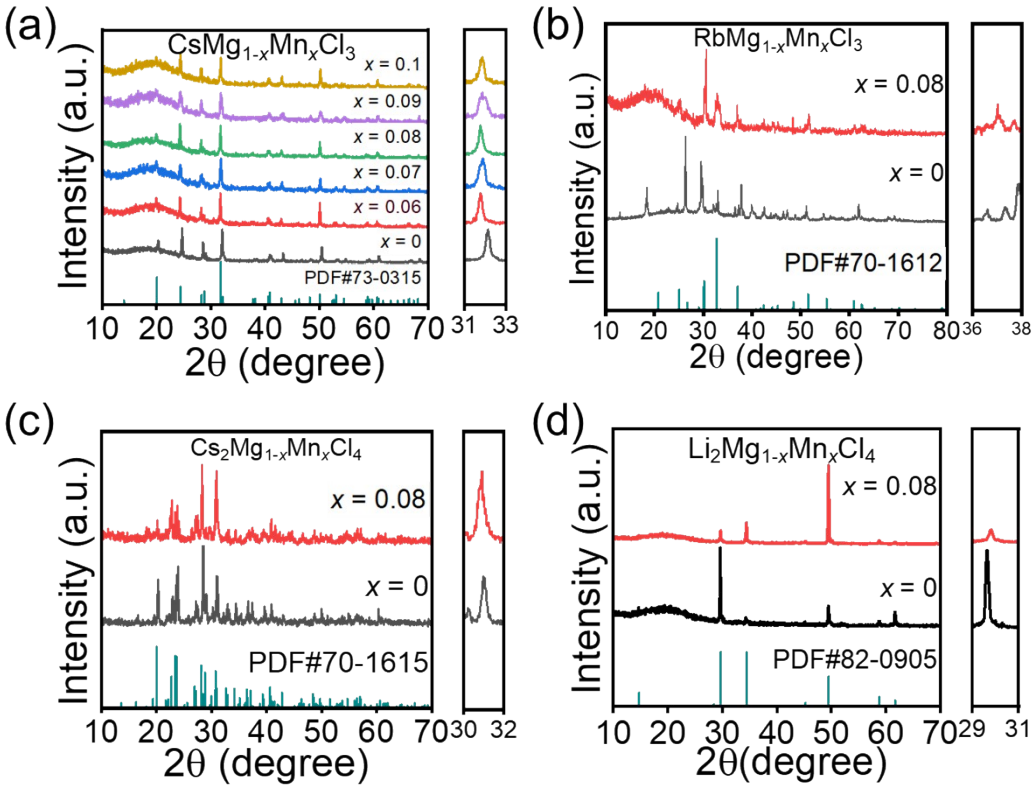

Figure S11. The PXRD patterns of (a) $CsMg_{1-x}Mn_xCl_3$ ($x = 0 – 0.1$), (b) $RbMg_{1-x}Mn_xCl_3$ ($x = 0/0.08$), (c) $Cs_2Mg_{1-x}Mn_xCl_4$ ($x = 0/0.08$) and (d) $Li_2Mg_{1-x}Mn_xCl_4$ ($x = 0/0.08$) were compared with standard cards.

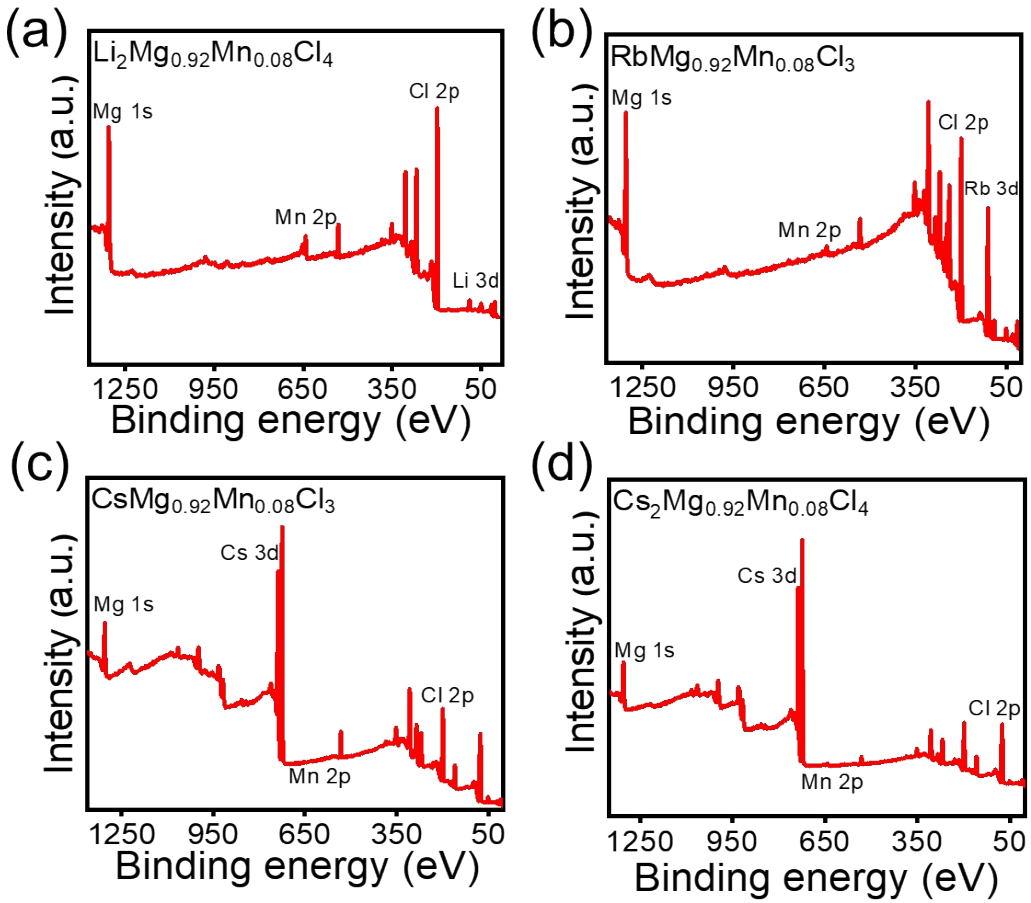

Figure S12. X-ray photoelectron spectra of (a) $Li_2Mg_{0.92}Mg_{0.08}Cl_4$, (b) $RbMg_{0.92}Mg_{0.08}Cl_3$, (c) $CsMg_{0.92}Mg_{0.08}Cl_3$ and (d) $Cs_2Mg_{0.92}Mg_{0.08}Cl_4$.

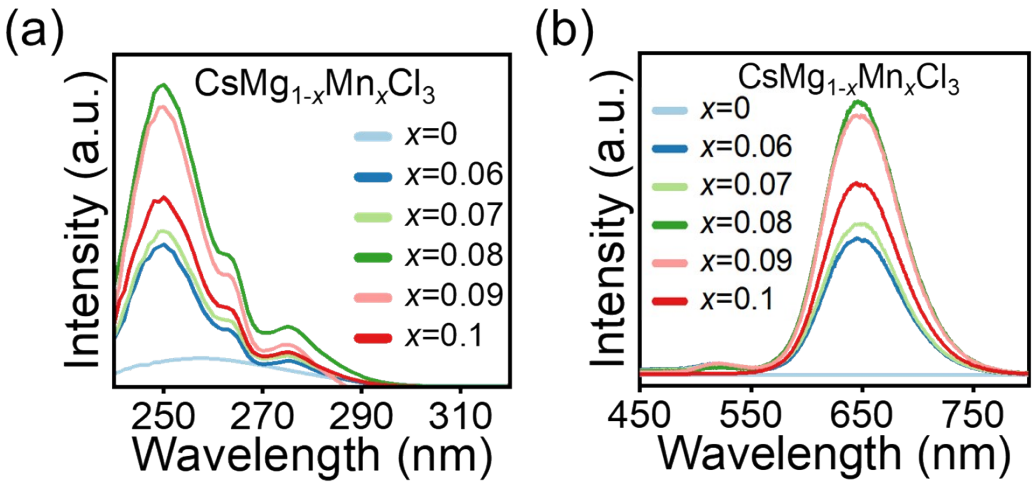

Figure S13. (a) and (b) are PLE and PL spectra of $CsMg_{1-x}Mn_xCl_3$ (x = 0 – 0.1).

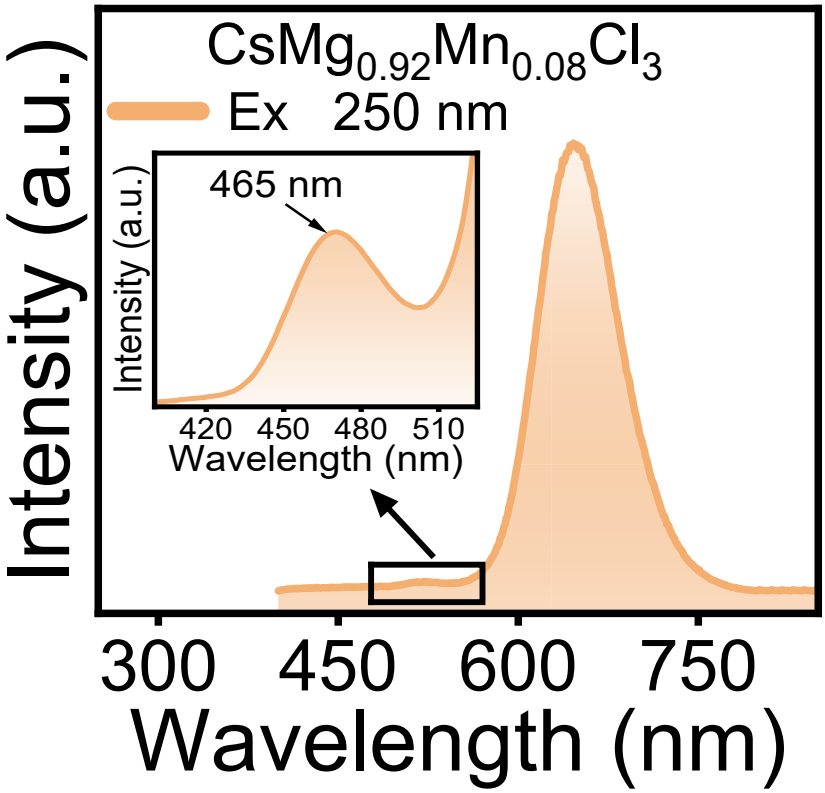

Figure S14. PL spectra of as-prepared $CsMg_{0.92}Mn_{0.08}Cl_3$ powders. (The inset is a magnified spectrum from 400 nm to 520 nm.)

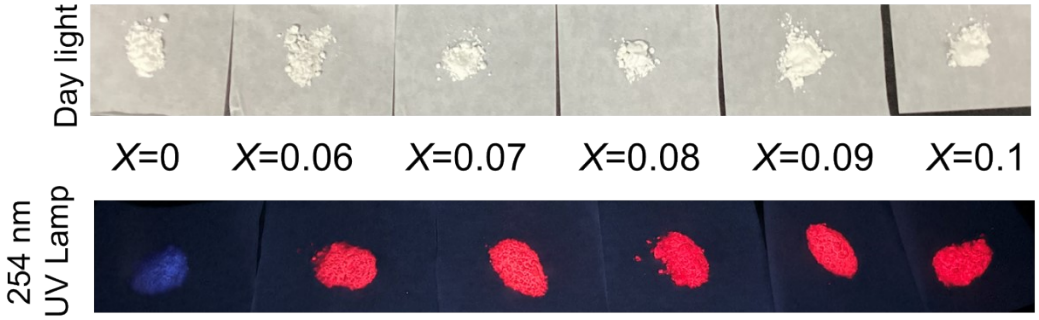

Figure S15. Luminescence contrast images of $CsMgCl_3$ with different Mn(II) ions doped concentrations under natural light and 254 nm UV lamp excitation were compared.

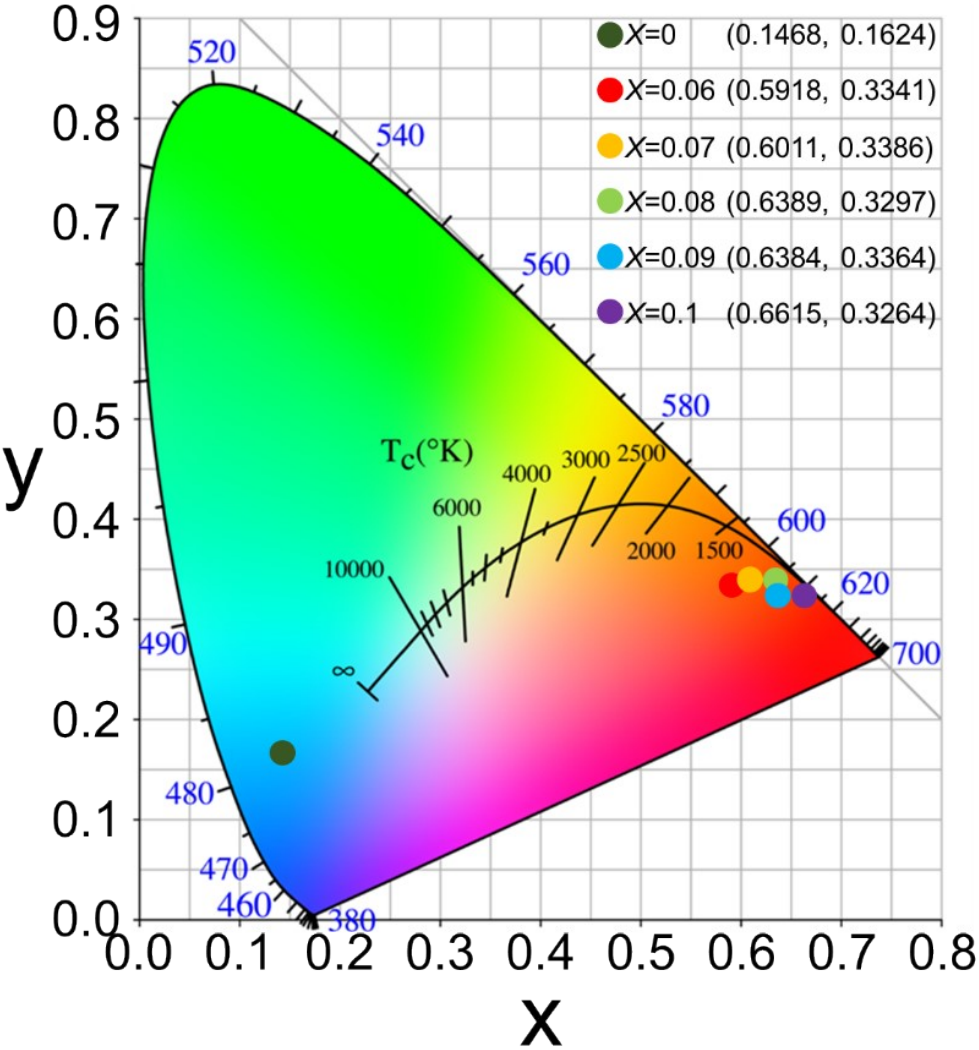

Figure S16. CIE chromaticity coordinates of $CsMg_{1-x}Mn_xCl_3$ (x = 0 – 0.1) displays.

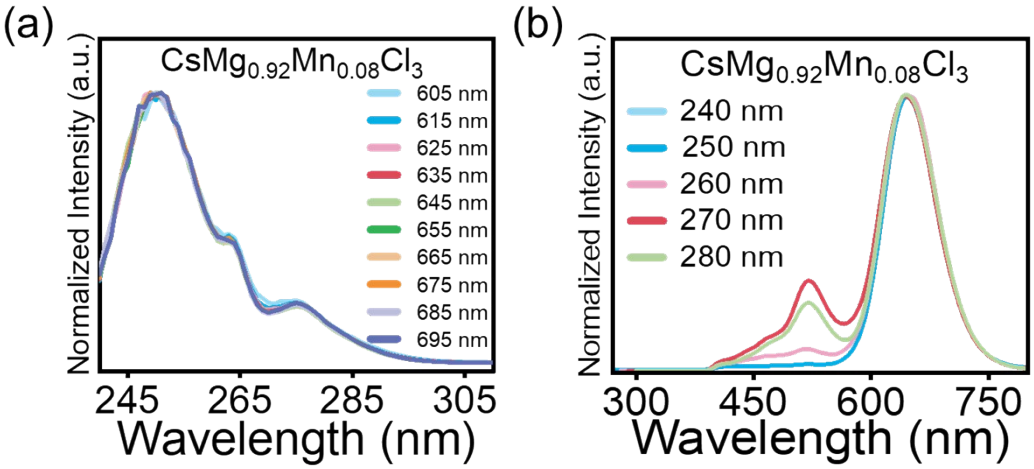

Figure S17. (a) Normalized PLE spectra of $CsMg_{0.92}Mn_{0.08}Cl_3$ were measured at different emission wavelengths in the range of 605 nm - 695 nm. (b) Normalized PL spectra of $CsMg_{0.92}Mn_{0.08}Cl_3$ at different excitation wavelengths were measured in the range of 240 nm - 280 nm.

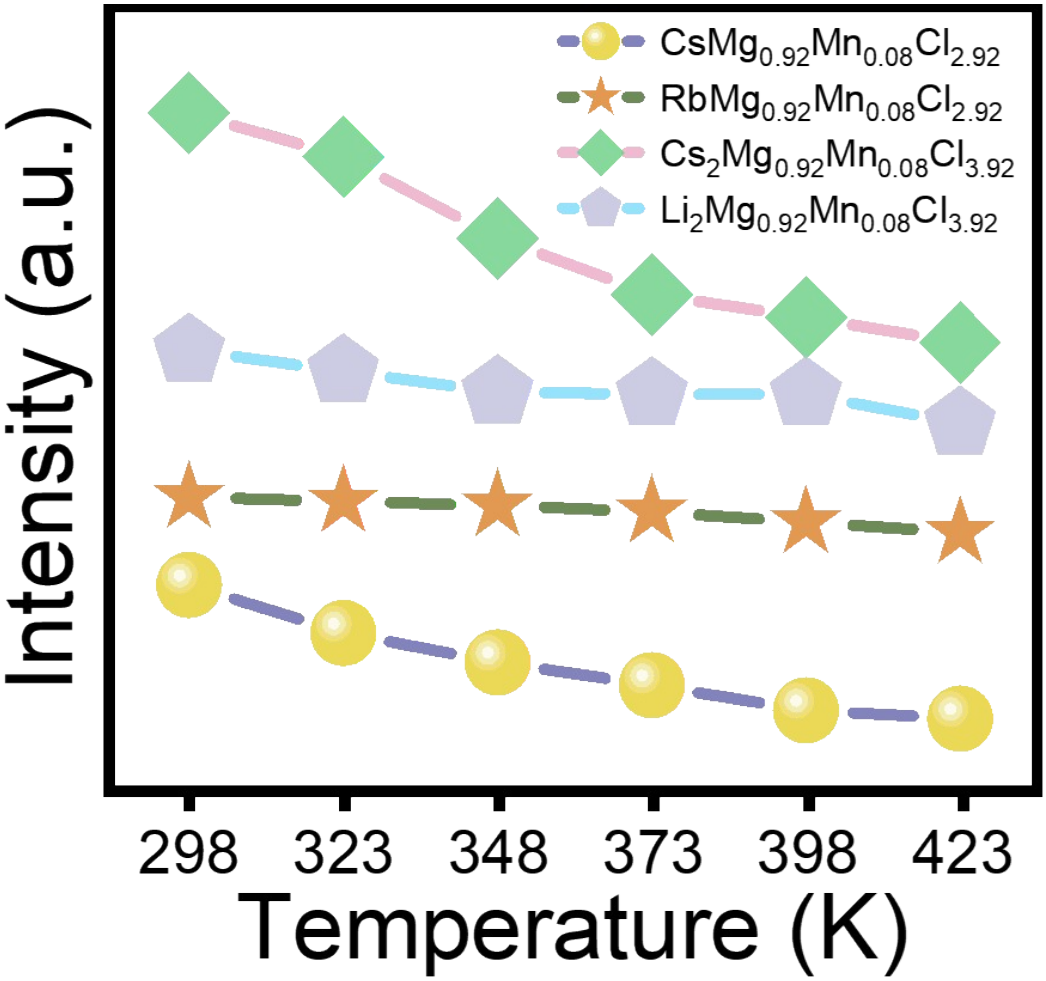

Figure S18. Comparison of variable temperature luminescence intensity of Mg halides.

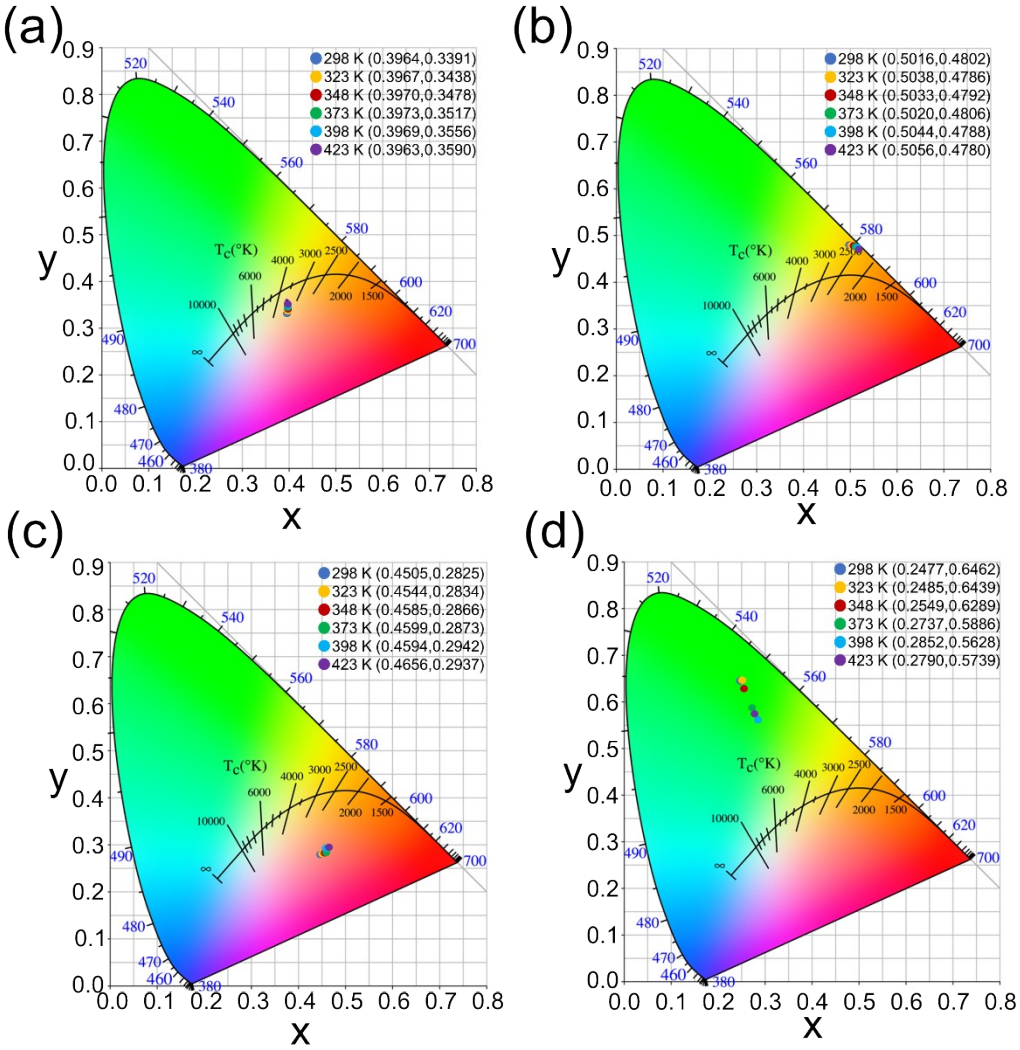

Figure S19. The CIE coordinates of PL in (a) $Li_2Mg_{0.92}Mg_{0.08}Cl_4$, (b) $RbMg_{0.92}Mg_{0.08}Cl_3$, (c) $CsMg_{0.92}Mg_{0.08}Cl_3$ and (d) $Cs_2Mg_{0.92}Mg_{0.08}Cl_4$ at different temperatures.

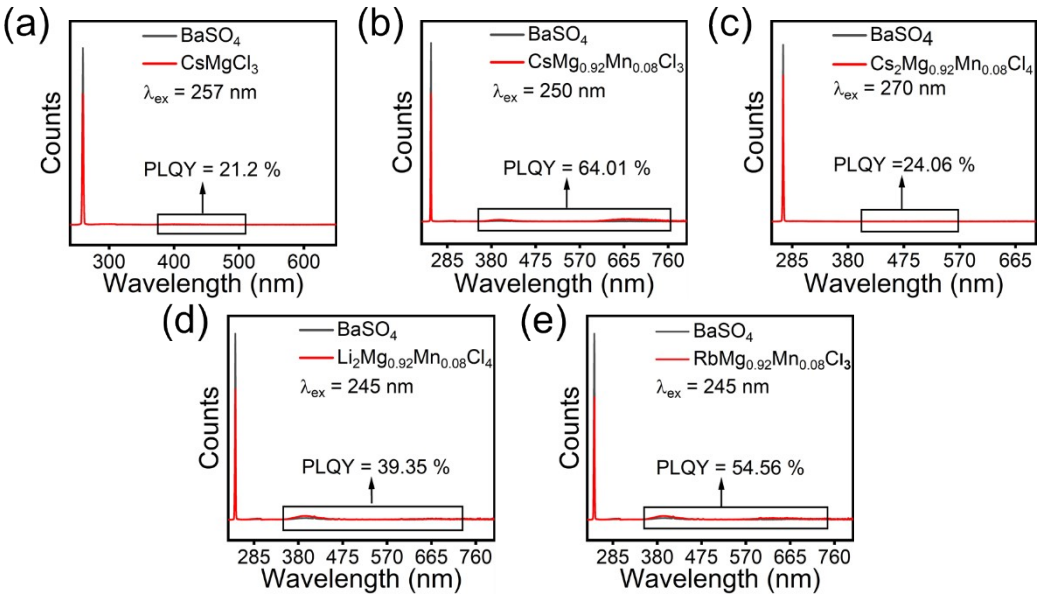

Figure S20. The result of PLQY measurements for (a) $CsMgCl_3$, (b) $CsMg_{0.92}Mn_{0.08}Cl_3$, (c) $Cs_2Mg_{0.92}Mn_{0.08}Cl_4$, (d) $Lis_2Mg_{0.92}Mn_{0.08}Cl_4$ and (e) $RbMg_{0.92}Mn_{0.08}Cl_3$.

Table S1. The comparison of the activation energy for the Mg halides and some well-known metal halides

S.No	Phosphor compositions	Activation energy E_a(eV)	Reference
1	$CsMnCl_3$	0.11	[1]
2	$CsCdCl_3$	0.62	[2]
3	$MAPbI_3$	0.32	[3]
]4	$[C_6H_7ClN]CdCl_3$	0.11	[4]
5	$Cs_2CaCl_4 \cdot 2H_2O$	0.45	[5]
6	$[PPh_3H]_2[SbCl_5]$	0.58	[6]
7	$CsMgCl_3$	0.37	This work
8	Cs_2MgCl4	0.19	This work
9	$RbMgCl_3$	0.27	This work
10	Li_2MgCl_4	0.31	This work

Table S2. The cell parameters of the Mg halides.

Samples	Space group	a (Å)	b (Å)	c(Å)	α(°)	β(°)	γ(°)	Z	Cell volume (Å^3)
$CsMgCl_3$	$P6_3/mmc$	7.260	7.260	6.170	90	90	120	2	282.09
$CsMg_{0.94}Mn_{0.06}Cl_3$	$P6_3/mmc$	7.267	7.267	6.181	90	90	120	2	282.65
$CsMg_{0.93}Mn_{0.07}Cl_3$	$P6_3/mmc$	7.273	7.273	6.189	90	90	120	2	283.12
$CsMg_{0.92}Mn_{0.08}Cl_3$	$P6_3/mmc$	7.279	7.279	6.191	90	90	120	2	283.30
$CsMg_{0.91}Mn_{0.09}Cl_3$	$P6_3/mmc$	7.281	7.281	6.193	90	90	120	2	283.45
$CsMg_{0.9}Mn_{0.1}Cl_3$	$P6_3/mmc$	7.289	7.289	6.201	90	90	120	2	283.78
$RbMgCl_3$	$P6_3/mmc$	7.095	7.095	17.578	90	90	120	6	766.31
$RbMg_{0.92}Mn_{0.08}Cl_3$	$P6_3/mmc$	7.125	7.125	17.589	90	90	120	6	766.48
Cs_2MgCl_4	Pnma	7.514	9.777	13.234	90	90	90	4	972.23
$Cs_2Mg_{0.92}Mn_{0.08}Cl_4$	Pnma	7.626	9.790	13.244	90	90	90	4	972.31
Li_2MgCl_4	Fd-3m	10.401	10.401	10.401	90	90	90	8	1125.19
$Li_2Mg_{0.92}Mn_{0.08}Cl_4$	Fd-3m	10.413	10.413	10.413	90	90	90	8	1125.68

1. Meng, Q.; Chen, L.; Jing, L.; Pang, Q.; Zhang, J. Z., Enhancing photoluminescence of manganese chloride perovskite-analogues through phase transformations induced by Sn incorporation. *Journal of Luminescence* **2023,** *255*, 119613.
2. Chakchouk, N.; Almalawi, Dhaifallah R.; Smaili, Idris H.; Aljuaid, F.; Rhaiem, Abdallah B., Investigation of Charge Transfer Mechanism and Dielectric Relaxation in $CsCdCl_3$ Perovskite. *Applied Organometallic Chemistry* **2025,** *39* (3), e7871.
3. Patel, V.; Sorathia, k.; Unjiya, K.; Patel, R.; Pandey, S. V.; Kalam, A.; Prochowicz, D.; Akin, S.; Yadav, P. K., Machine Learning-Driven Analysis of Activation Energy for Metal Halide Perovskites. *Dalton Transactions* **2025**.
4. Xu, H.; Zhang, Z.; Dong, X.; Huang, L.; Zeng, H.; Lin, Z.; Zou, G., Corrugated 1D Hybrid Metal Halide $[C_6H_7ClN]CdCl_3$ E xhibiting Broadband White-Light Emission. *Inorganic Chemistry* **2022,** *61* (11), 4752-4759.
5. Wang, H.; Pan, Y.; Ding, Y.; Lian, H.; Lin, J.; Li, L., Tunable Multicolor Emission and High Thermal Stability in Single-Matrix Luminescent Crystals Based on Calcium Perovskites for Advanced Solid-State Lighting Applications. *Advanced Optical Materials* **2024,** *12* (24), 2400935.
6. Peng, Y.-C.; Zhou, S.-H.; Jin, J.-C.; Zhuang, T.-H.; Gong, L.-K.; Lin, H.-W.; Wang, Z.-P.; Du, K.-Z.; Huang, X.-Y., $[PPh_3H]_2[SbCl_5]$: A Zero-Dimensional Hybrid Metal Halide with a Supramolecular Framework and Stable Dual-Band Emission. *The Journal of Physical Chemistry C* **2022,** *126* (40), 17381-17389.